SCIENCE CHINA
Earth Sciences

Progress of Projects Supported by NSFC
• REVIEW •

December 2012 Vol.55 No.12: 1929–1941
doi: 10.1007/s11430-012-4532-y

Deep carbon recycling and isotope tracing: Review and prospect

ZHANG HongMing[1*] & LI ShuGuang[2,1]

[1] *Science Research Institute, China University of Geosciences, Beijing 100083, China*;
[2] *CAS Key Laboratory of Crust-Mantle Materials and Environments, School of Earth and Space Sciences, University of Science and Technology of China, Hefei 230026, China*

Receive February 20, 2012; accepted August 27, 2012

Deep carbon recycling is an essential part of the global carbon cycle. The carbonates at the bottom of the ocean are brought to the mantle by subduction. Subsequently, deep carbon is released to the atmosphere in the form of CO_2 through volcanism. At present, research on deep carbon recycling is still at its early stage. The proportion of subduction-related carbon and primary mantle-derived carbon in CO_2 released by volcano is an important issue. Carbon isotopes can easily distinguish organic carbon from inorganic carbon. However, ~95% of subduction-related and primary mantle-derived carbon released by volcano is inorganic, which carbon isotopes find difficult to distinguish. Recently, Ca and Mg isotope geochemistry has provided important tools for tracing crust-derived material recycling. Here we focus on this topic by introducing the principles of C, Ca, and Mg isotopes in tracing deep carbon recycling and previous research results. We also summarize the research progress on the total storage and phases of deep carbon, CO_2 fluxes which depend on the release via volcanism, the partial melting of the carbon-bearing mantle, and carbon behaviour during oceanic subduction.

deep carbon, carbon recycling, Ca isotope, Mg isotope

Citation: Zhang H M, Li S G. Deep carbon recycling and isotope tracing: Review and prospect. Sci China Earth Sci, 2012, 55: 1929−1941, doi: 10.1007/s11430-012-4532-y

Global carbon cycle is an essential part of earth system science, particularly because CO_2 balance in the atmosphere is a key factor affecting the Earth's climate. Thanks to the increasing concern on global warming and carbon abatement, the study of the carbon cycle has received much attention. The carbon cycles are divided into two parts, namely, surface carbon and deep carbon cycles. Water cycle and the carbon cycle are essential parts of the Earth's surface system. In fact, both extend into the Earth's interior [1]. Surface carbon cycle (atmosphere-hydrosphere-biosphere) has been well studied in recent years [2]. In geological time, carbonates at the bottom of the ocean are brought to the mantle via subduction, and then released to the atmosphere in the form of CO_2 through volcanism. This process is called deep carbon recycling.

At present, research on deep carbon recycling is still at its early stage. Deep carbon recycle study involves a series of scientific issues, including the total storage of deep carbon, fluxes of deep carbon recycling, phases of deep carbon, the partial melting of the carbon-bearing mantle, the release of CO_2 fluxes to the atmosphere by volcanism, and the proportion of subduction-related carbon and primary mantle-derived carbon in total CO_2 released by volcanism. Among those, the last one is the most important scientific issues. Carbon isotopes may be used to easily distinguish organic carbon from inorganic carbon. However, ~95% of subduction-related carbon and primary mantle-derived carbon among the total CO_2 released by volcanism is inorganic; hence, carbon isotopes cannot be used to distinguish subduction-related carbon from primary mantle-derived carbon

*Corresponding author (email: zhm003210501@yahoo.cn)

[3].

Nowadays, increasing attention has been given to Ca and Mg isotopes, as new developed isotope systems for using in tracing crust-derived material cycle [4, 5]. A large amount of Ca and Mg is stored in carbon-rich oceanic sediments and basalts. The Ca-Mg isotopic composition of sediments is significantly different from that of the mantle. Thus, Ca-Mg isotopes may be used to trace the subduction-related carbon in mantle-derived rocks, providing crucial evidence in solving some scientific issues. The present paper focuses on the following aspects: the total storage of deep carbon, fluxes of deep carbon recycling, phases of deep carbon, the partial melting of the carbon-bearing mantle, CO_2 fluxes released to the atmosphere by volcanism, previous research results in the field of isotopes, and the potential application of tracing deep carbon recycling using Ca-Mg isotopes.

1 Amount of carbon stored in the mantle

Identifying the content of carbon in the mantle is important in understanding the deep carbon recycling, because it is apparently related to the total amount of the carbon. Researchers have conducted studies on this issue [6–11]. However, different researchers obtained different values, which ranged from 20–1300 ppm [12]. This inconsistency is due mainly to the different samples used, along with the varied degassing models used under different systems. Thus, the simulation results only represent the local reservoir. Despite the differences, there are two most widely used methods: a two-step Rayleigh fractionation model and the magmatism model.

1.1 Two-step Rayleigh fractionation model

The first step in this model is the release of CO_2 under a decompression condition, accompanied by the rising magma and the decrease in CO_2 solubility. In this step, the Rayleigh fractionation model between CO_2 and magma is used. The second step is the continuous release of CO_2 during the rise of magma. In this step, the open system model is used in the degassing process between the previous stage and the later one.

For the closed system, take Cartigny et al. [7] as an example, the degassing model is as follows:

$$\frac{C_i^{\text{melt}}}{C_i^0} = \left(\frac{\rho S_i \cdot T_C / T_0}{V^* + \rho S_i \cdot T_C / T_0} \right),$$

in which C_i^{melt} is the concentration of carbon in the melt, C_i^0 is its initial concentration, S_i is its solubility, V^* is the vesicularity, ρ is the melt density and T_C and T_0 are the closure and standard temperatures, respectively. An open system is decomposed into several closed systems. Based on the previous closed system, C_i^0 is replaced by the residual volatile concentration. It would then approximate successively to the concentration in the source [7].

1.2 Magmatism model

Bureau et al. [6] measured the carbon concentration of melt inclusions and fluid inclusions in the Piton de la Fournaise volcano olivine phenocrysts, which could reach nearly 520 ppm at most. Carbon is an incompatible element in the peridotite-basalt magma system; hence, its partition coefficient is very low (D_{CO2} <<1). The carbon concentration of the source regions is calculated according to classical batch equilibrium partial melting, which ranges from 63–277 ppm.

Additionally, many researchers use CO_2-to-incompatible element (or other volatile components) ratio to estimate carbon concentrations in the mantle [7, 8, 10, 11], which change very little during the magma process. For example, Saal et al. [8] found a linear relationship between CO_2 contents and Nb abundances in undegassed mid-ocean ridge basalt samples (CO_2/Nb = 239 ± 46). The result indicates that, under the undegassed condition, CO_2 may be regarded as incompatible; such incompatibility maintains a constant ratio with Nb. The Nb concentration for the mantle source is 0.3 ± 0.05 ppm; accordingly, the CO_2 concentration is 72 ± 19 ppm. This method should receive more attention, because it is not available for all mantle sources. First, the CO_2-to-Nb ratio of a series of samples should be studied. Subsequently, the correlation between CO_2 and Nb may be observed.

Hirschmann and Dasgupta [13] systematically studied carbon concentration for the depleted mantle and enriched mantle using the H/C ratio. H_2O and CO_2 are both volatile components, and have similar chemical behaviors. They used the simple classic batch equilibrium partial melting model to simulate H/C for the source, which is 0.75 ± 0.25 and 0.5 ± 0.3 for MORB and OIB, respectively. In addition to the H concentration, they finally acquired the carbon concentration for the depleted mantle and enriched mantle, namely, 16 ± 9 and 33–500 ppm, respectively. The total carbon budget for the mantle is (0.8–12.5) × 10^{23} g (Figure 1). The mass of the Earth is ~6.0×10^{27} g [14]. The average content of the Earth is 730 ppm [15], so the total carbon budget for the Earth is estimated at 4.4 × 10^{24} g. The budget for the mantle accounts for 1.8 wt% to 28.4 wt% of the total Earth budget. No detailed study about the proportion of depleted mantle and enriched mantle exists; hence, the difference between the maximal estimated value and the minimal one is almost an order of magnitude. Thus, further information about tectonic settings worldwide is needed. Subsequently, a three-dimensional model of the carbon concentration for the mantle may be set up under a global scale; however, much work needs to be done. The advantage of the magmatism model is that it has been studied perfectly. However, its results are in a very large error when used in

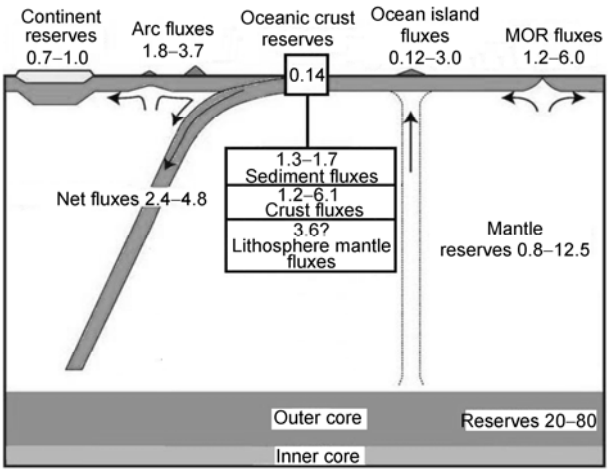

Figure 1 Total budget of mantle carbon ($\times 10^{23}$ g) and fluxes of deep carbon ($\times 10^{13}$ g/yr) . Modified after Dasgupta and Hirschmann[12].

an open system. In contrast, the Rayleigh fractionation model may be used well in an open system. However, other ways need to be used to study the magma degassing process.

2 Phases of deep carbon

Carbon is stored abundantly in the mantle; thus, it comes in different forms. This topic includes two issues: the phase of carbon in the mantle and the phase of carbon in the magma.

2.1 Phase of carbon in the mantle

Carbon in the solid mantle exists mainly in the inclusions and a small amount in mineral cracks and gaps among minerals [3]. Carbon has very low solubility in silicate minerals. The carbon concentrations for olivine and pyroxene are lower than 12 ppmw (1–11 GPa) and 200 ppbw (1.5 GPa), respectively [16]. Based on the oxidation and reduction valence state, carbon-bearing accessory minerals have mainly three forms: oxidized carbon; neutral carbon; and reduced carbon. These forms have been discussed in detail. Thus, we only provide a simple table herein (Table 1). Aside from the mantle, carbon is also stored in $(Fe, Ni)_7C_3$ in the core [12].

The phase of carbon in the mantle is controlled by temperature, pressure, and oxygen fugacity. Temperature has little effect on the solid carbonate multi-phase transition, although it mainly controls the carbonate solubility and melting. High temperature and pressure experiments are discussed in detail below. The two biggest factors are pressure and oxygen fugacity.

2.1.1 Pressure

The value of oxygen fugacity is large, with a depth less than 120 km (pressure less than 4 GPa). Thus, almost all of the carbon present is oxidized to carbonates. Pressure is the most important factor under such condition, which causes calcite [17] and solid carbonate multi-phase transitions. Carbonate in the mantle often has many components, and isomorphism often occurs among the cations. The carbon-bearing phases in the mantle are shown in Figure 2. With increasing pressure, carbonate becomes more Ca-rich, but less Mg-rich.

Table 1 Oxidation states and chemical and mineralogical forms of carbon in the mantle[a)]

Oxidized State	Species	forms
Oxidized C	CO_2	CO_2 in fluid inclusions
	carbonate	calcite, dolomite and magnesite
Neutral C	graphite	mineral surfaces, and in cracks as grains
	diamond	inclusion in kimberlites, lamproites, UHPM rocks
	solid solution C	in the crystal lattice of silicates
	organic compounds	on cracks and mineral surfaces and in inclusions
	gaseous Species	in fluids inclusions
Reduced C	SiC	in kimberlite matrix and inclusion in diamond

a) Modified after Deines [3]

2.1.2 Oxygen fugacity

The most important factor is the oxygen fugacity when the depth becomes larger than 120 km. Oxygen fugacity controls the valence state of carbon. Under high oxygen fugacity conditions, carbon is oxidized into carbonate or CO_2. On the contrary, when oxygen fugacity becomes low, neutral or reduced, carbon becomes CH_4 or SiC. Woodland and Koch [34] showed that mantle oxygen fugacity decreases with increasing pressure. Carbonates are not stable at depths greater than ~120 km (~4 GPa) in the subcratonic and asthenospheric mantle [35, 36], and are reduced to neutral carbon (e.g. diamond) [37]. Rohrbach and Schmidt [37], meanwhile, discovered that oxygen fugacity affects the phase of carbon under the condition (P = 10–23 GPa; T = 1400–1900°C). They used carbonated peridotite as samples and multianvil devices to generate high pressure.

Their result shows that, under high oxygen fugacity conditions (f_{O_2}= IW +4 to +5), carbon is stored almost entirely in carbonate, that is, it is almost magnesite. However, carbonate becomes unstable when oxygen fugacity is low (f_{O_2}< IW + 1.2), and will be reduced to neutral carbon. Micron-size diamond has been observed. The reaction is as follows:

$$MgCO_3 + 2(Fe,Ni)_0 = 3(Fe, Ni, Mg)\,O + C$$

When carbonate is reduced to neutral carbon, it cannot easily participate in the magma process. The melting point of diamond is higher than 3500°C [38]. Under this condition, carbon is redox freezing. When other geological processes increase oxygen fugacity, carbon is activated and continued

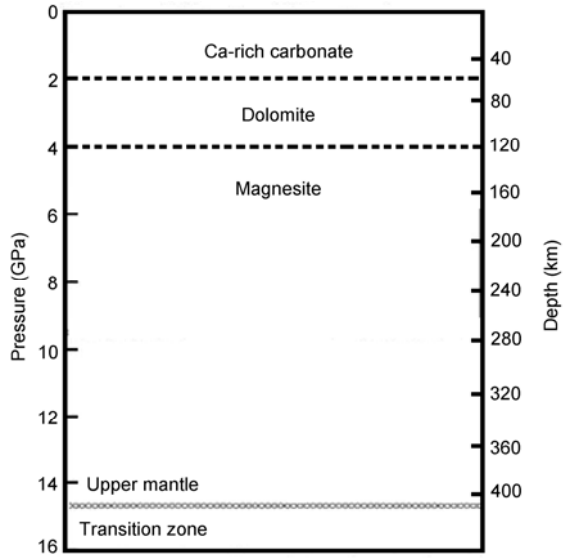

Figure 2 Carbon-bearing phases in the mantle. From refs. [18–33].

to participate in the recycling.

2.2 Phases of carbon in magma

Magma eruption is the main way to transport deep carbon to the Earth's surface. The phase of carbon in magma depends on the concentration of alkali metal elements [39]. CO_2 dissolves solely as carbonate groups in basanite, leucitite and nephelinite magmas [39]. In intermediate composition magma (andesite), CO_2 dissolves not only as carbonate minerals, but also as CO_2 molecules [39]. All CO_2 dissolve solely as CO_2 molecules in rhyolite magma [39].

Dixon [40] defined a compositional parameter Π that takes into account the roles of Si^{4+}, Al^{3+}, Ca^{2+}, K^+, Na^+, Mg^{2+}, and Fe^{2+} cation fractions:

$$\Pi = -6.50\,(Si^{4+} + Al^{3+}) + 20.17\,(Ca^{2+} + 0.8K^+ + 0.7Na^+ + 0.4Mg^{2+} + 0.4Fe^{2+}).$$

At 0.1 GPa and 1200°C, the description of CO_2 solubility in basalt melts of variable alkalinity gives the following equation [41]:

$$CO_2\ (\text{ppm}) = 920\ (\pm 1)\ \Pi - 17(\pm 53),\ R^2 = 0.89.$$

This linear relationship can be used to predict CO_2 solubility of basaltic magmas of different alkali contents at 1200°C and 0.1 GPa. However, there are not enough data to test the applicability at other temperature and pressure [41].

3 Carbon behaviour during oceanic crust subduction

Large amounts of carbonates are stored in oceanic sediments. Along with subduction, 1.4×10^{15} g/yr of sediments are taken into the deep Earth [42], including a large amount of carbon. An important issue is the change in carbon behavior during the subduction process. Would the carbonate minerals stored in the sediments be stable during this process? Would CO_2 be released during this process? Will carbonate melt be released during the subduction process? One of the most important ways to solve such problems is to perform the high *P* and high *T* experiments to model the carbonate multi-phase transition during the subduction process [43].

Many researchers have performed this kind of experiment [19–21, 26, 33]. Although they have different results, they all concluded that the release of sedimentary carbonates is unlikely in modern subduction zones and would enter the deep continuously. In the experiment conducted by Dasgupta et al. [26], eclogite xenolith was used as the sample. The rock powder was dried overnight at 1000°C in a CO/CO_2 gas mixing furnace. Then it was added a mixture of synthetic (reagent grade Na_2CO_3, K_2CO_3 and $CaCO_3$) and natural (magnesite and siderite) carbonates. Experiments were performed in a piston cylinder (PC, 2.0–3.3 GPa) and multi-anvil (MA, 3.3–8.5 GPa) devices.. The purpose of this experiment is to obtain the solidus of carbonated eclogite; hence, detecting the onset of partial melting in our experiments is essential. Quenched carbonatitic melt has been observed in triple grain junctions and along the grain edges between the silicate phases, which may be considered as the ideal sample to reach the solidus.

The experimental results are as follows: the carbonate decomposed the volatile CO_2 under the condition (P = 3 GPa; T = 1000°C). Thus, carbonate-rich magma, which reaches a depth of ~100 km, would be broken down to release CO_2 gas. As the pressure grows continuously to 2–4 GPa, calcite turns into dolomite. When the pressure reaches 4.5–5 GPa, the dolomite would decompose, and generate magnesite (Figures 3 and 4). The lowest temperature for carbonate solidus range from 1020°C to 1050°C at a pressure of 3–5 GPa. This would continue to increase with the increase in pressure (Figure 3).

Comparing this solidus with the *P-T* conditions for subducting oceanic crust shows that the solidus cannot intersect with the *P-T* curve of subduction (Figure 4), even under the hottest subducting condition. The carbonate carried by subduction of oceanic crust cannot easily produce carbonatite magma. Additionally, oxygen fugacity is low in the deep mantle, carbonate is reduced to neutral C [37]. And thus, it is harder to melt.

Although carbonatite is not easily produced during oceanic crust subduction, fluids that come from the metamorphic or dehydrated process may dissolve part of the carbonate, which can then be carried into the mantle wedge and finally released by OIB. Thus, input fluxes into the mantle are different from initial carbon recycling fluxes. Decarbonation efficiency describes the ratio between fluxes of carbon released by OIB and those of carbon carried into the mantle.

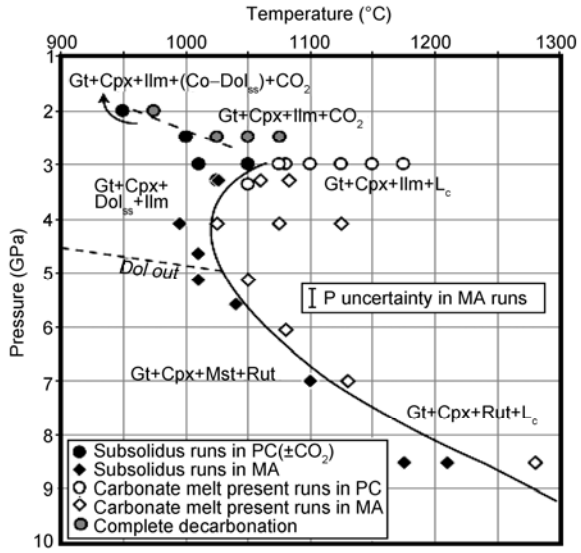

Figure 3 Phase diagram of carbonated eclogite. After Dasgupta et al. [26].

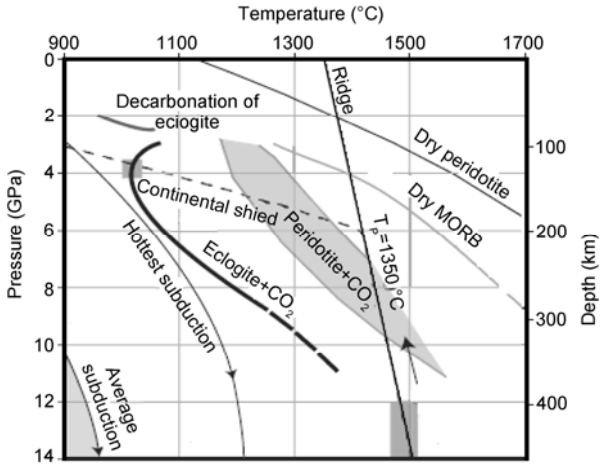

Figure 4 Carbonated eclogite solidus in relation to the different tectonic geotherms. After Dasgupta et al. [27].

Johnston et al. [44] studied the relationship between the ages of subducting oceanic crusts with their decarbonation efficiencies (Figure 5), and found that subducting oceanic crusts are smaller than 20% crusts when the ages are younger than 20 Ma. However, the cool crust older than 40 Ma show decarbonation efficiencies more than 50%. For very few example, the efficiency of Lesser Antilles with age is 70 Ma accounts for 65% (Figure 5). It is opposite to our speculation by theory. In the Archean the mantle potential temperature was higher than that in modern; hence, their efficiency was quite high [12]. Most carbon cannot be carried into the mantle and released to the atmosphere when the shallow mantle is deficient in carbon [12]. For this case, Johnston et al. [44] also explained that younger crust in higher temperature geotherms significant dehydration occurs at fore arc depths, which causes serpentinite to form in the cold corner of the mantle wedge, since temperatures are too cold for partial melting to occur. However, dehydration of cooler slabs occur at sub-arc depths so that the carbon can enter the system. Although given significant variations in the decarbonation efficiencies of hot slabs and cool slabs, ~50% of the total carbon can enter the deep mantle via oceanic crust subduction.

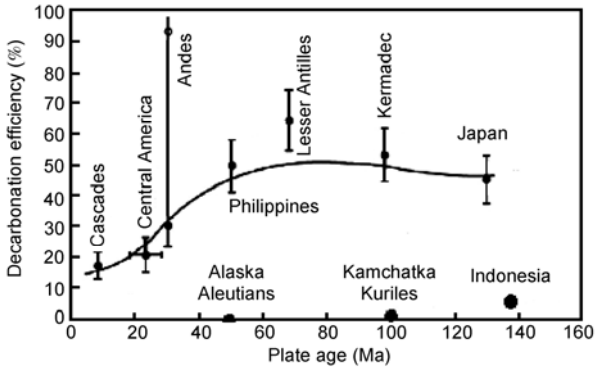

Figure 5 Decarbonation efficiency versus age of subducting slab. After Johnston et al. [44].

4 Melting of carbon-bearing mantle

Similar to water, a small amount of CO_2 may also cause the solidus temperature to decrease substantially due to its volatility. The present research on this issue is similar with that on carbonate behaviour during the process of oceanic crust subduction, which is discussed above. They are both performed under the condition of high *P-T*. The samples are slightly different. The former is carbonated eclogite, whereas the later is carbonated peridotite or an artificial mixture with similar components (CaO-MgO-Al_2O_3-SiO_2-CO_2 ± Na_2O ± FeO* ± other oxide systems) [18, 27, 28].

Many experimental petrologists performed similar research using different pressures: P = 3.0–10.0 GPa [27]; P = 10.0–20.0 GPa [31]; and P = 10.5–32.0 GPa [32]; P=10.0, 14.0, 23.0 GPa [37]. Dasgupta and Hirschmann [12] gathered the results and obtained a carbonated peridotite solidus. The solidus, over the pressure range of 2–35 GPa, is given by:

$$T=0.024\times P^3-2.21\times P^2+73.8\times P+830.4.$$

The blue line in Figure 6 is the solidus line obtained by fitting the experimental data. Notably, the experimental data are abundant at $P \leqslant 20.0$ GPa. Thus, the corresponding solidus is very well constrained (solid line). However, only three data exist at P>20.0 GPa [12]; hence, the corresponding solidus lacks constraints, which is speculative (dotted line). Rohrbach and Schmidt [37] tested the carbonated

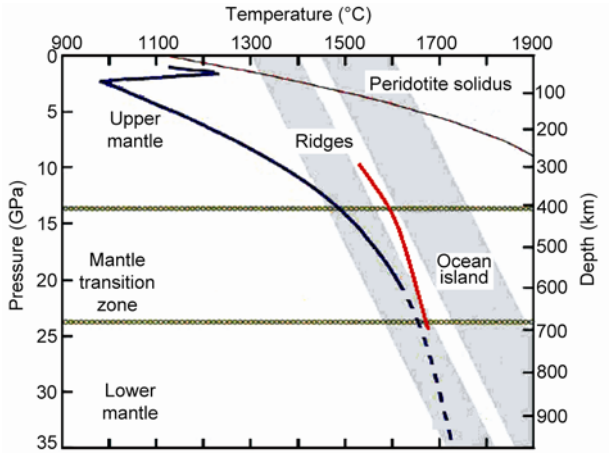

Figure 6 Experimental constraints on the solidus of carbonated peridotite. Blue line comes from Dasgupta and Hirschmann [12]; red line comes from Rohrbach and Schmidt [37]. Modified after Dasgupta and Hirschmann [12].

mantle peridotite solidus temperature at P = 10.0, 14.0 and 23.0 GPa, and fit another section of solidus line (red line). The solid line is longer than before and could be found a certain gap between two lines at P = 10.0 GPa. However, the blue solid line obtained by Dasgupta and Hirschmann [12] is a fitting function which is also different from the actual data. This issue needs more research.

The intersection point of the mantle adiabat and the carbonated peridotite solidus shows that the generation of carbonatitic melt may occur at a depth of 300–600 km, which is 300 km deeper than that of pure peridotite. What this means is that when the upwelling of magma reaches 300–600 km, the carbonated peridotite begins to melt. However, the melting pure peridotite may occur at a depth less than 100 km with decreasing pressure.

The above discussion is based on the condition of high oxygen fugacity, which is low in the deep mantle. The carbonate would thus be reduced to neutral carbon (diamond) or reduced carbon (carbide). Two possibilities may occur: the mantle peridotite would melt, but carbon would not (carbon would be carried as an inclusion to the surface, such as diamond in kimberlite); or with the increasing melts, neutral carbon (diamond) or reduced carbon (carbide) would be oxidized to carbonate, which would then melt. The latter possibility depends on the redox conditions. Thus, the solidus in Figure 6 should be revised. Oxidizing reactions [12] of neutral carbon or carbide may occur as follows:

$$C + Mg_2SiO_4 + O_2 = MgCO_3 + MgSiO_3$$

$$C + 3FeSiO_3 + 2Fe_2O_3 = FeCO_3 + 3Fe_2SiO_4$$

$$2Fe_3C + 4FeSiO_3 + 5O_2 = 2FeCO_3 + 4Fe_2SiO_4$$

$$Fe_7C_3 + 30FeSiO_3 + 13Fe_2O_3 = 3FeCO_3 + 30Fe_2SiO_4$$

Carbon is in the form of diamond or graphite; Mg_2SiO_4 and Fe_2SiO_4 are in the form of olivine or wadsleyite (a polymorph of olivine at high pressure); $MgSiO_3$ is in the form of low-Ca pyroxene or pyroxene, with the structure of perovskite; $FeSiO_3$ is in the form of orth pyroxene or pyroxene, with the structure of perovskite; Fe_2O_3 is in the form of hematite with the structure of perovskite or hematite; $MgCO_3$ and $FeCO_3$ are melt; and Fe_3C and Fe_7C_3 are Fe-rich carbide.

Neutral carbon is oxidized to carbonate which would melt, thus changing the former solidus (Figure 7) because oxygen fugacity is low in the deep mantle. Carbon is in the form of diamond or carbide, which are difficult to melt. The only time they would melt is when they rise to the shallow surface and change into carbonate. Therefore, the solidus depends on the depth of the above oxidation reaction. However, due to the lack of detailed information of the deep mantle's oxygen fugacity, two redox melting lines are uncertain [12] (Figure 7). The partial melting of carbon-bearing mantle under different oxidized or reductive conditions could affect the degassing efficiency of CO_2, which is larger under oxidized conditions than under reductive conditions at a depth of more than 300 km [12].

5 Estimate on modern fluxes of carbon in and out of the mantle

Carbon on the Earth's surface is carried by oceanic crust subduction into deep mantle. Conversely, melting of the carbon-bearing mantle brings carbon back to the surface, of which there are two processes. However, which carbon flux is larger? Does the deep Earth store carbon for the surface or release carbon to the surface? This issue is evidently important, and thus, the modern fluxes of carbon need to be estimated in and out of the mantle.

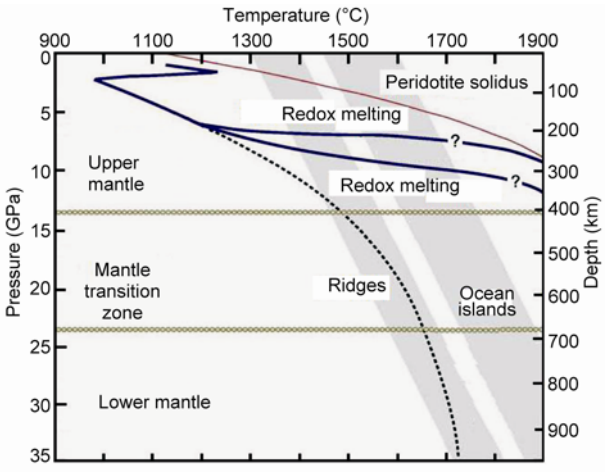

Figure 7 Experimental constraints on the solidus of carbonated peridotite under low oxygen fugacity condition. After Dasgupta and Hirschmann [12].

5.1 Carbon flux into the mantle by oceanic crust subduction

Based on its composition and carbon content, the subducting oceanic crust may be divided into three parts: (1) marine sediments; (2) basaltic oceanic crust; and (3) lithosphere mantle. The following formula is used for its estimation:

$$\text{Carbon flux} = \text{Subduction rate} \times \text{Thickness} \times \text{Density} \times \text{Carbon content}.$$

5.1.1 Marine sediments

Plank and Langmuir [45] collected deep-sea sediment samples, analyzed the type, density, and CO_2 content of sediments from each station, and studied the C flux into the mantle from each subduction zone and added them together to obtain the global C flux carried by ocean sediments into the mantle.

The principle of the method used is similar to that of the above formula. Due to different subduction zones, they added a variable that is the width of the subduction zones. $F = C_a \times t \times L \times \rho \times R$. C_a is the content of element a, t is the thickness of the sediments, L is the width, ρ is the density of sediment, and R is the subduction rate (km/yr). Finally, this formula is used to obtain the carbon flux, that is, 1.1×10^{13} g/yr.

5.1.2 Basaltic oceanic crust

The average CO_2 content of the typical 7 km thick basaltic oceanic crust is ~0.3 wt% [12]. The density is 2.86 ± 0.03 g/cm^3 [46]. The subduction rate is 3 km^2/yr [47]. The carbon flux of the basaltic oceanic crust into the mantle is 4.9×10^{13} g/yr, which is almost consistent with the 6.1×10^{13} g/yr estimated by Dasgupta and Hirschmann [12]. However, Dasgupta and Hirschmann [12] did not show the calculation in detail. Hence, the causes of the gap could not be identified easily.

5.1.3 Lithosphere mantle

Firstly, the carbon content for the lithosphere mantle must be obtained, as discussed above. Different researchers obtained different values. This inconsistency is due mainly to the different samples used, along with the varied degassing models used under different systems. However, it needs to be done on a global scale. The average carbon content for the upper mantle is about 14.4–60.0 ppm [48]. The density of the upper mantle is 3.3–3.4 g/cm^3 [49]. The subduction rate is also 3 km^2/yr. Given the average thickness of the lithosphere is 80 km, the carbon flux for the lithospheric mantle can be obtained, which is $(1.1–4.9) \times 10^{13}$ g/yr.

Three parts are added to obtain the total carbon flux for the subduction zone into the mantle, that is, $(7.1–10.9) \times 10^{13}$g/yr, within the range of $(6.1–11.4) \times 10^{13}$ g/yr (Figure 1) by Dasgupta and Hirschmann [12]. The reason of large range is the lack of accurate data.

5.2 Carbon flux to the atmosphere by volcanism

CO_2 content of the undegassing volcanic rocks is measured, which is substracted by the CO_2 content of the cooled rock after degassing, and then multiplied by the volume of the erupting magma. Finally, the fluxes of CO_2 released to the atmosphere by volcanism is acquired [50]. The channels of volcanism include mid-ocean ridges, arc volcanoes, and oceanic islands and plumes. Hayes and Waldbauer [50] used the results from Saal et al. [8] to show a linear relationship between CO_2 and Nb (CO_2/Nb = 239 ± 46). In accordance with the average Nb content of all MORBs source, which is 5.02 ppm, multiplied by 239, the CO_2 content for the initial MORB is 1200 ppm. The result is then subtracted by that of the cooled MORB, which is 200 ppm; hence, the CO_2 emission content is 1000 ppm. The volume of MORB increased by 21 km^3. Given the density of 2.8 g/cm^3, C flux to the atmosphere by MORB is 1.6×10^{13} g/yr. The C flux for arc volcanoes, and oceanic islands and plumes may also be obtained by this method; hence, 1.9×10^{13} [51] and 1.2×10^{13} g/yr [50], respectively.

The estimated results by Dasgupta and Hirschmann [12] are shown in Figure 1. The C flux for MORB is $(1.2–6.0) \times 10^{13}$ g/yr. The C flux for OIB is difficult to estimate accurately, because CO_2 is not totally released to the atmosphere and partly lost in sub-aerial intraplate eruptions [12]. Additionally, varying degrees of enrichment in the ocean island basalt source regions add to the difficulty of performing an estimation [12]. Dasgupta and Hirschmann [12] assumed that the C flux for OIB is $(0.12–3.0) \times 10^{13}$ g/yr, that is, 10%–50% of that for MORB. For Arc, the precious estimation [48, 51, 52] may be smaller. However, fluxes not associated with volcanoes (such as metamorphic fluids) are not considered, which may also lead to significant volatile that may also contain CO_2 transport from the slab to the surface [53]. In addition, the CO_2 out flux related to magmatic intrusion is unconstrained [12]. The primary island arc volcanic magma may have higher CO_2 content than that we estimated before [54].

In brief, estimation of carbon fluxes in and out of the mantle is imprecise. The balance of the carbon cycle between the Earth's surface and the deep mantle is not clear. Although some uncertainties exist, Dasgupta and Hirschmann [12] estimated that the present-day net flux of carbon into the mantle could reach 3.1×10^{13} g/yr, at most. Compared with carbon flux to the atmosphere by volcanism and the total carbon budget of the mantle, Dasgupta and Hirschmann [12] suggested that the residence time of carbon in the mantle is >1 Ga and perhaps as long as 4.6 Ga.

Whether or not the carbon released by volcanoes is subduction-related carbon, its proportion is needed for observation and proof of the isotopic tracer. Recycled carbon is generally in the form of carbonate (Ca, Mg, and Fe) CO_3 that consists mainly of five elements. From traditional stable isotopes, carbon isotopes have more potential than oxy-

gen isotopes. On one hand, C isotopes can trace recycled biogenic organic carbon [55]. On the other hand, magma fractional crystallization can lead to O isotopes fractionation [56]. From non-traditional stable isotopes, Mg and Ca isotopes have more potential than Fe isotopes, because Fe isotopes fractionate during magmatic processes under present analysis precision [57, 58]; however, Mg and Ca do not [59–61]. At present, no detailed research on Fe or O isotopes tracing deep carbon recycling exists. The present paper focuses on tracing the deep carbon recycling using C, Mg, and Ca isotopes.

6 Carbon isotopes tracing deep carbon recycling

6.1 Carbon isotopes of diamond in kimberlite

Carbon isotopes could easily distinguish organic and inorganic carbon, because the δ^{13}C (‰ relative to PDB) of organic carbon is lower than –15, whereas that of inorganic carbon is higher than –10 [3, 62, 63]. If the mantle-derived rocks or the inclusions have δ^{13}C lower than –15, their sources must contain abundant crustal material, because no organism has been found in the mantle. Bulanova et al. [55] studied the carbon isotopic composition of the diamond in the Collier 4 kimberlite pipe from Juina in Brazil. They found that the δ^{13}C of a group of diamonds' cores is lower than –20. They conclude that these diamonds contain evidence of subducted oceanic sediment contamination. Walter et al. [64] also studied the carbon isotopes of diamond in the Juina-5 kimberlite pipe and found that part of the diamond's δ^{13}C is lower than –15, and may reach –24.1, at lowest. The petrology study on mineral inclusions shows that diamond comes from the lower mantle, and provides direct geochemical evidence for oceanic crust subduction into the lower mantle. Moreover, such study also makes the deep carbon cycle extend to the lower mantle.

6.2 Joint carbon and noble gas isotope tracing deep carbon cycle—the proportion of crust-derived recycling carbon and primitive mantle-derived carbon from volcanic gases

The helium isotopic compositions of the crust and the upper mantle are quite different. The ^{3}He/^{4}He of the continental crust and the MORBs are approximately < 0.1 Ra and 8.0–9.0 Ra, respectively [65]. Helium isotopes can trace crust-derived material contamination. Sano and Marty [66] applied He-C isotopes to set up three components of the mixing model (limestone–sedimentary organic C–mantle C) (Figure 8). The three equations are as follows:

$$(^{13}C/^{12}C)_{Obs} = (^{13}C/^{12}C)_{MORB} \times M + (^{13}C/^{12}C)_{Lim} \times L + (^{13}C/^{12}C)_{Sed} \times S,$$

$$1/(^{12}C/^{3}He)_{Obs} = M/(^{12}C/^{3}He)_{MORB} + L/(^{12}C/^{3}He)_{Lim} + S/(^{12}C/^{3}He)_{Sed},$$

$$M + L + S = 1.$$

Subscript Obs, MORB, Lim, and Sed represent the observation samples, mid-ocean ridge basalt, sedimentary limestone (marine carbonates) and sedimentary organic C, respectively. M, L, and S represent each proportion. In addition, $(^{13}C/^{12}C)_{MORB}=1.1147\times10^{-2}$; $(^{13}C/^{12}C)_{Lim}=1.1220\times10^{-2}$; $(^{13}C/^{12}C)_{Sed}=1.0883\times10^{-2}$; $(^{12}C/^{3}He)_{MORB}=1.5\times10^{9}$; $(^{12}C/^{3}He)_{Lim}=1.0\times10^{13}$; and $(^{12}C/^{3}He)_{Sed} = 1.0\times10^{13}$. Based on the above three equations, the proportion of the three ends of volcanic gases could be determined. Elemental fractionation of the $CO_2/^3$He ratio and isotopic fractionation of the $^{13}C/^{12}C$ ratio are not significant in crater samples at relatively high temperature. Take Sano et al. [67] as an example, they tested the helium and carbon isotopes of CO_2 from the crater fumaroles of Galeras volcano, Colombia. The containers are pre-evacuated lead glass with vacuum stopcocks at both ends. The gases were introduced into the container directly from the fumaroles. After several minutes of collecting, he closed the stopcocks. Applied to the above equation, most Galeras volcano gases were derived from limestone carbon including slab component, and only 3%–10% came from MORB-type mantle. Here $CO_2/^3$He replaces $^{12}C/^3$He, because carbon isotopes fractionate little under relative high terperature.

CO_2 from the deep Earth (e.g., the mantle) is released to the atmosphere. Aside from volcanoes, other processes, such as deep faults and microleakages, exist. These processes may release CO_2, but have no magmatic activity. Under this condition, only the gas geochemical methods can be used to study the deep carbon cycle, such as the He iso-

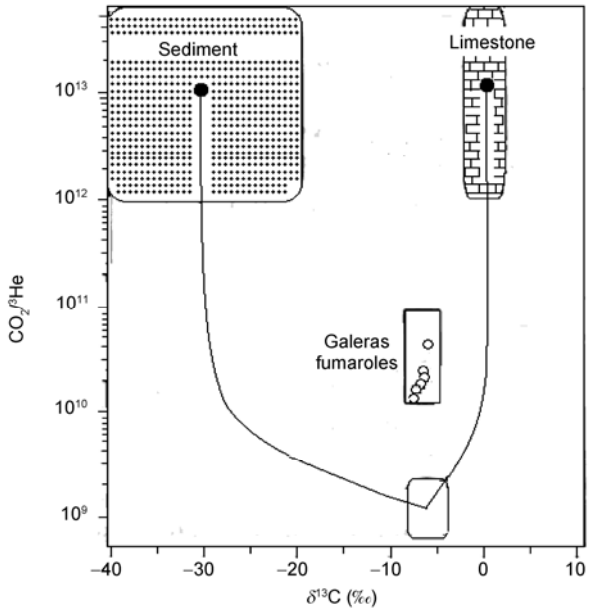

Figure 8 Three-component mixing model (limestone-sedimentary organic carbon-mantle carbon) for Galeras volcanic gases based on $CO_2/^3$He ratio and carbon isotopic composition. Modified after Sano et al. [67].

tope [68]. The disadvantage of this method is that it is suitable for younger volcanic rocks. However, it is not suitable for the intrusive rocks and older rocks that may experience gas dissipation; hence, misapplication may lead to large errors in the results.

Volcano gases derived from different sources may contaminate CO_2 stored in the crust, which does not participate in the deep carbon recycling and is not a component of the cycle. Only subduction-related carbon and the primary mantle-derived carbon make up the essential part of this cycle. As mentioned above, using carbon isotopes to distinguish the carbon derived from different sources may be difficult; noble gas isotopes need to be combined. Compared with directly testing noble gas isotopes of volcano gases, Ca-Mg isotopes in mantle-derived magma have more advantages in this aspect.

7 Ca-Mg isotopes tracing crust-derived materials recycling

7.1 Principle of Mg isotopes tracing deep carbon recycling

7.1.1 Mg isotopic composition of oceanic carbonate

Every year, 5×10^{12} kg $CaCO_3$ precipitates are detected in the ocean worldwide (a total of 60% forms sediments, whereas the other 40% are dissolved). Nearly half of the precipitates are found in coral reefs, inshore, and in the tropical continental shelf. Most $CaCO_3$ precipitated in the ocean is made up of foraminifera and coccolithophores [69], which play an important role in the Mg isotopic composition of subduction carbonate. Chang et al. [70] reported the Mg isotopic composition of foraminifera. Different species of foraminifera have different Mg isotopic compositions δ^{26}Mg ($\delta^{26}\text{Mg} = [(^{26}\text{Mg}/^{24}\text{Mg})_{\text{Sample}}/(^{26}\text{Mg}/^{24}\text{Mg})_{\text{Standard}}-1] \times 1000$. The standard is DSM3 [71]). However, the difference is small, δ^{26}Mg = –6.19 to –4.18. Meanwhile, Wombacher et al. [72] reported the Mg isotopic composition of biological samples from different sea area. δ^{26}Mg for foraminifera and coccolith ooze are –5.57 to –2.48 and –3.05 to –1.04, respectively.

In summary, the oceanic sedimentary carbonate enriches more light Mg isotopes compared with the typical mantle rocks.

7.1.2 Mg isotope fractionation caused by the dehydration process of subduction

With increasing temperature and pressure, the oceanic crust undergoes a blueschist-amphibolite-eclogite facies metamorphism. During this process, carbonated basalts undergo metamorphism and dehydration. An important issue is whether or not Mg isotopes would fractionate during this process, this is a question that needs to be addressed first.

Li et al. [73] studied the Mg isotopic composition of whole-rock eclogite from Bixiling, Dabie Orogen, China. They suggested δ^{26}Mg = –0.44 to –0.26, which is the mantle-like Mg isotopic compositions, to be the limited Mg isotope fractionation during eclogite-facies metamorphism. However, protoliths of Bixiling eclogites are gabbro cumulates [74, 75] that have low water content and cannot represent dehydration during the subduction. Thus, a series of representative HP-UHP metamorphic rocks need to be collected from the subducting oceanic crust. Afterwards, their Mg isotopic composition, which undergoes various metamorphic facies, must be analyzed. The present work has yet to be done and is worthy of more in-depth research.

7.1.3 Research case of Mg isotopes tracing deep carbon recycling

Yang et al. [76] systematically studied the Mg isotopic composition of Mesozoic and Cenozoic basalts in the North China Craton. They divided the basalts into two groups based on their ages. One group was older than 120 Ma, whereas the other was younger than 110 Ma. The isotopic composition (δ^{26}Mg = –0.31 to –0.25, with an average of –0.27 ± 0.05 (2 SD) of the first group is similar to that of the mantle. However, the isotopic composition of the second group of basalts (δ^{26}Mg = –0.60 to –0.42), with an average of –0.46 ± 0.10 (2SD) is lower than that of the first group. In addition, the second group of basalts is Ca-enriched.

The modeling result shows that the lighter isotopic composition of the second group of basalts is likely caused by recycled oceanic sediment carbonates that have been carried by the subducting oceanic crust. This group also has some geochemistry characteristics that are similar to that of the HIMU component, considered the recycled subducting oceanic crust. Therefore, Yang et al. [76] concluded that low δ^{26}Mg in the second group of basalts from Eastern North China Craton, with ages younger than 110 Ma, is caused by the mantle magma source mixed with recycled carbonate rocks carried by the subducted oceanic crust.

7.2 Principle of Ca isotope tracing deep carbon cycle

7.2.1 Ca isotopic composition of oceanic carbonate

Inorganic carbon in the sediments is carried by the subducting oceanic crust. CaO content of the sediments [45] is higher than that of the mantle [77]. Therefore, using Ca isotopes to trace deep carbon cycle would be more efficient. The mass-dependent Ca isotopic variations are expressed as δCa. $\delta^{x/y}\text{Ca}=[(^{x}\text{Ca}/^{y}\text{Ca})_{\text{样品}}/(^{x}\text{Ca}/^{y}\text{Ca})_{\text{标样}}-1] \times 1000$. The standard is NIST SRM 915a [78], where x is 42 or 44, and y is 40 or 42. The $\delta^{44/40}$Ca of ancient oceanic sediments is usually less than 0.5 (e.g., ref. [79, 80]), whereas that of lithosphere and the typical mantle is 1.05 ± 0.04 [61, 81–83]. Mixed with oceanic carbonate, $\delta^{44/40}$Ca of the igneous rocks could be low, which may trace crust-derived carbonate ma-

terial contamination.

7.2.2 Research case of Ca isotopes tracing deep carbon recycling

Huang et al. [4] recently studied the Ca isotope composition of Hawaiian shield stage tholeiites and found that Hawaiian plume is mixed with ancient carbonate. They analyzed the Ca isotopic composition of 10 samples from 4 sites and found that $\delta^{44/40}$Ca = 0.75–1.02 is significantly lower than that of typical upper mantle, which is 1.05 ± 0.04. However, $\delta^{44/40}$Ca of ancient carbonate is usually less than 0.5. They also compared the $\delta^{44/40}$Ca with the content of CaO, Sr/Nb, and $^{87}Sr/^{86}Sr$, and found that $\delta^{44/40}$Ca-Sr/Nb and $\delta^{44/40}$Ca-$^{87}Sr/^{86}Sr$ have a negative correlation (Figure 9). This result indicates that tholeiites have lower $\delta^{44/40}$Ca with more ancient carbonates mixed into them. Furthermore, the modeling result shows that the source of Hawaiian basalt is mixed with 4% ancient carbonate.

7.3 Difference of Mg and Ca isotopes tracing deep carbon recycling

The basic principles of the isotope tracer of the deep carbon recycling involve the differences that exist between the Ca-Mg isotopic composition of the Earth's surface sediments and typical mantle. This difference may be tested accurately through mass spectrometry. The Mg and Ca isotope compositions of the Earth's surface sediments may change over time. In geological time, the Mg and Ca isotopic compositions of oceanic sediments are different from those of modern oceanic sediments.

The $\delta^{44/40}$Ca of ancient oceanic carbonate (limestone and dolomite) is usually less than 0.5. That of modern oceanic carbonates (limestone and dolomite) is in general larger than 0.5 but with considerable variations [84, 85]. As mentioned above, 60% of $CaCO_3$ precipitates in the ocean worldwide form sediments, whereas the remaining 40% is dissolved. Nearly half of the precipitates are in the coral reefs, inshore, and the tropical continental shelf. Most $CaCO_3$ precipitated in the ocean forms foraminifera and coccolithophores, playing an important role in the Mg isotopic composition of subduction carbonate. When $CaCO_3$ is precipitated from seawater, it preferentially take up light Ca isotopes from seawater, which makes the seawater's Ca isotopes heavier [86] (Figure 10). Ca isotopes have more advantage in tracing ancient sedimentary carbonate contamination than the modern.

Currently, the varying Mg isotopic compositions of oceanic carbonates during geological time has not been well studied. However, this topic is worthy of further study. Mg isotopic composition of the modern oceanic carbonate is lower than that of the typical mantle. Light Mg isotope is enriched in $CaCO_3$ [72]. Therefore, the isotopic composition of the ancient oceanic carbonate may be lower than that of the modern carbonate, and those of the ancient oceanic carbonate and the typical mantle differ significantly. Mg isotopes can trace the contamination of oceanic sediment with any age. However, the high MgO content of the mantle [77] can more easily dilute that of the carbonate, which does not makes it as sensitive as Ca isotopes.

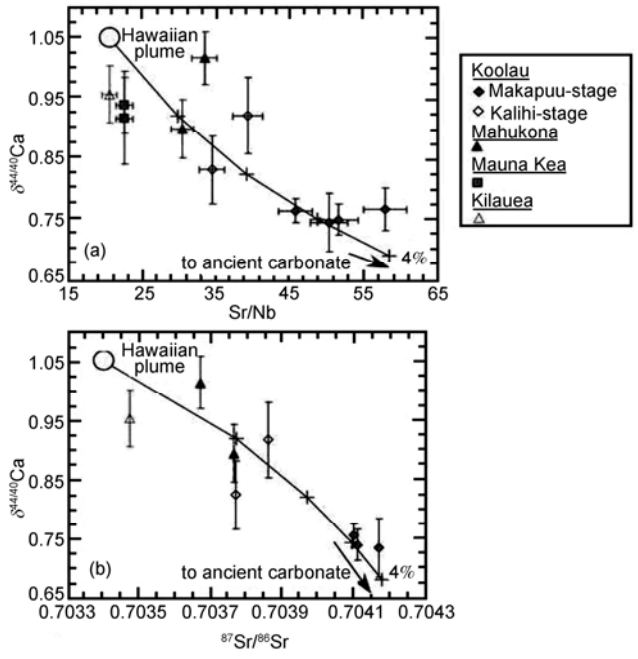

Figure 9 $\delta^{44/40}$Ca vs. Sr/Nb and $^{87}Sr/^{86}Sr$ in Hawaiian tholeiites. After Huang et al. [4].

8 Prospect

The deep carbon recycling is an essential part of the global carbon cycle. Carbonates at the bottom of the oceanic plate are brought to the mantle by subduction, followed by its release in the form of CO_2 to the atmosphere through vol-

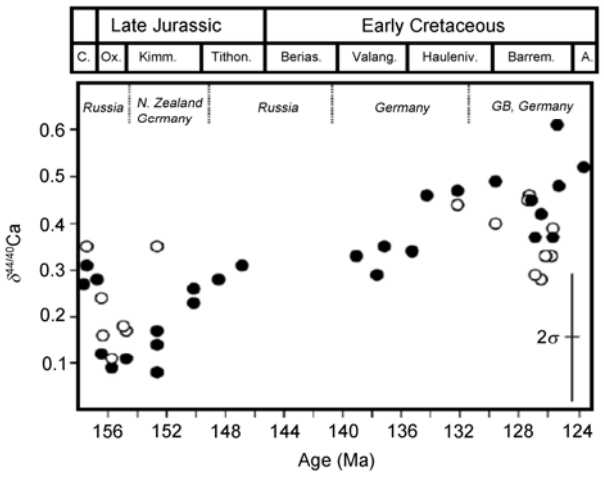

Figure 10 $\delta^{44/40}$Ca of the Middle Jurassic to Early Cretaceous belemnites as determined by TIMS and MC-ICP-MS. Filled circles come from TIMS; open circles come from MC-ICP-MS. After Farkaš et al. [79].

canism. In turn, this forms the carbon cycle between the deep Earth and its surface. With the subducting plate cooling, the carbon content of the modern mantle may be higher than that of the ancient, which is important in knowing the regulation on the evolution of CO_2 content. Research on the budget of deep carbon and its phase has achieved a large number of results. However, research on deep carbon recycling is still at its early stage, and deserves more attention. The following scientific issues should be given further attention in future studies.

(1) For the total budget of deep carbon, the difference between the maximal and the minimal estimated value is almost an order of magnitude. More information is needed to obtain the precise value. The change in budget in geological times is still an important part of the deep carbon recycling.

(2) Aside from the release of CO_2 and the production of carbonatitic magma, carbonate solution is a way of decarbonation during the subduction process. However, no detailed experimental data on carbonate solution under high *P-T* exist; furthermore, there is no way to draw the carbonate solubility curve under different temperatures and pressures.

(3) Research on Ca-Mg isotope tracing the deep carbon recycling has made initial progress. However, many issues need to be studied, such as whether or not the Mg isotopic composition of oceanic carbonate changes with time. Do the Ca and Mg isotopes fractionate during the process of HP-UHP metamorphism and dehydration? Do differences exist in Ca-Mg isotopic tracing, and does this tracing under different geological backgrounds, and so on?

(4) To understand the effect of the deep carbon recycling on CO_2 in the atmosphere, an accurate estimation of the proportion of subduction-related carbon and primary mantle carbon must be done. Joint C-He isotope tracing is one of the ways to explore this issue. However, more experiments are needed.

(5) Volcanic magma and its contained gas may be derived from the same or different sources. The mobility of CO_2 gas in a volcano is quite large for the open magmatic system, which may be derived from a different source from the magma. Mg and Ca isotopes mainly trace carbon in magma, which is not exactly equivalent to the carbon in the volcanic gas. Tracing the deep carbon recycling by Mg and Ca isotopes is still at its early stage. The relationship between the two different derived carbon has yet to be studied and is, therefore, worthy of further research.

Fang Huang and two reviewers are thanked for their comments and suggestions. This study was supported by National Natural Science Foundation of China (Grant Nos. 40973016, 41230209).

1 Wang P X. Earth system science in China quo vad is (in Chinese)? Adv in Earth Sci, 2003, 18: 837–851
2 Qu J S, Sun C Q, Zhang Z Q, et al. Trends and advances of the global chance studies on carbon cycle (in Chinese). Adv in Earth Sci, 2003, 18: 980–987
3 Deines P. The carbon isotope geochemistry of mantle xenoliths. Earth Sci Rev, 2002, 58: 247–278
4 Huang S C, Farkaš J, Jacobsen S B. Stable calcium isotopic compositions of Hawaiian shield lavas: Evidence for recycling of ancient marine carbonates into the mantle. Geochim Cosmochim Acta, 2011, 75: 4987–4997
5 Li W Y, Teng F Z, Ke S, et al. Heterogeneous magnesium isotopic composition of the upper continental crust. Geochim Cosmochim Acta, 2010, 74: 6867–6884
6 Bureau H, Pineau F, Métrich N, et al. A melt and fluid inclusion study of the gas phase at Piton de la Fournaise volcano (Réunion Island). Chem Geol, 1998, 147: 115–130
7 Cartigny P, Jendrzejewski N, Pineau F, et al. Volatile (C, N, Ar) variability in MORB and the respective roles of mantle source heterogeneity and degassing: The case of the Southwest Indian Ridge. Earth Planet Sci Lett, 2001, 194: 241–257
8 Saal A E, Hauri E H, Langmuir C H, et al. Vapour undersaturation in primitive mid-ocean-ridge basalt and the volatile content of Earth's upper mantle. Nature, 2002, 419: 451–455
9 Aubaud C, Pineau F, Hékinian R, et al. Degassing of CO_2 and H_2O in submarine lavas from the Society hotspot. Earth Planet Sci Lett, 2005, 235: 511–527
10 Cartigny P, Pineau F, Aubaud C, et al. Towards a consistent mantle carbon flux estimate: Insights from volatile systematics (H_2O/Ce, δD, CO_2/Nb) in the North Atlantic mantle (14°N and 34°N). Earth Planet Sci Lett, 2008, 265: 672–685
11 Shaw A M, Behn M D, Humphris S E, et al. Deep pooling of low degree melts and volatile fluxes at the 85°E segment of the Gakkel Ridge: Evidence from olivine-hosted melt inclusions and glasses. Earth Planet Sci Lett, 2010, 289: 311–322
12 Dasgupta R, Hirschmann M M. The deep carbon cycle and melting in Earth's interior. Earth Planet Sci Lett, 2010, 298: 1–13
13 Hirschmann M M, Dasgupta R. The H/C ratios of Earth's near-surface and deep reservoirs, and consequences for deep Earth volatile cycles. Chem Geol, 2009, 262: 4–16
14 Yoder C F. Astrometric and geodetic properties of Earth and the solar system. In: Ahrens T J, ed. Global Earth Physics: A Handbook of Physical Constants, AGU Reference Shelf. Washington D C: American Geophysical Union, 1995. 1–31
15 McDonough W F. Compositional Model for the Earth's Core. In: Holland H D, Turrekian K K, eds. Treatise on Geochemistry. Amsterdam: Elsevier, 2004. 547–568
16 Shcheka S S, Wiedenbeck M, Frost D J, et al. Carbon solubility in mantle minerals. Earth Planet Sci Lett, 2006, 245: 730–742
17 Liu L G, Mernagh T P. Phase transitions and Raman spectra of calcite at high pressures and room temperature. Am Mineral, 1990, 75: 801–806
18 Dalton J A, Presnall D C. Carbonatitic melts along the solidus of model lherzolite in the system CaO-MgO-Al_2O_3-SiO_2-CO_2 from 3 to 7 GPa. Contrib Mineral Petrol, 1998, 131: 123–135
19 Hammouda T. High-pressure melting of carbonated eclogite and experimental constraints on carbon recycling and storage in the mantle. Earth Planet Sci Lett, 2003, 214: 357–368
20 Yaxley G M, Brey G P. Phase relations of carbonate-bearing eclogite assemblages from 2.5 to 5.5 GPa: Implications for petrogenesis of carbonatites. Contrib Mineral Petrol, 2004, 146: 606–619
21 Dasgupta R, Hirschmann M M, Dellas N. The effect of bulk composition on the solidus of carbonated eclogite from partial melting experiments at 3 GPa. Contrib Mineral Petrol, 2005, 149: 288–305
22 Thomsen T B, Schmidt M W. Melting of carbonated pelites at 2.5–5.0 GPa, silicate-carbonatitie liquid immiscibility, and potassium-carbon metasomatism of the mantle. Earth Planet Sci Lett, 2008, 267: 17–31
23 Wallace M E, Green D H. An experimental determination of primary carbonatite magma composition. Nature, 1988, 335: 343–346
24 Falloon T J, Green D H. The solidus of carbonated, fertile peridotite.

Earth Planet Sci Lett, 1989, 94: 364–370
25 Falloon T J, Green D H. Solidus of carbonated fertile peridotite under fluid-saturated conditions. Geology, 1990, 18: 195–199
26 Dasgupta R, Hirschmann M M, Withers A C. Deep global cycling of carbon constrained by the solidus of anhydrous, carbonated eclogite under upper mantle conditions. Earth Planet Sci Lett, 2004, 227: 73–85
27 Dasgupta R, Hirschmann M M. Melting in the Earth's deep upper mantle caused by carbon dioxide. Nature, 2006, 440: 659–662
28 Dasgupta R, Hirschmann M M. Effect of variable carbonate concentration on the solidus of mantle peridotite. Am Mineral, 2007, 92: 370–379
29 Dasgupta R, Hirschmann M M. A modified iterative sandwich method for determination of near-solidus partial melt compositions. II. Application to determination of near-solidus melt compositions of carbonated peridotite. Contrib Mineral Petrol, 2007, 154: 647–661
30 Brey G P, Bulatov V K, Girnis A V, et al. Experimental melting of carbonated peridotite at 6–10 GPa. J Petrol, 2008, 49: 797–821
31 Ghosh S, Ohtani E, Litasov K D, et al. Solidus of carbonated peridotite from 10 to 20 GPa and origin of magnesiocarbonatite melt in the Earth's deep mantle. Chem Geol, 2009, 262: 17–28
32 Litasov K D, Ohtani E. Solidus and phase relations of carbonated peridotite in the system CaO-Al_2O_3-MgO-SiO_2-Na_2O-CO_2 to the lower mantle depths. Phys Earth Planet Interiors, 2009, 177: 46–58
33 Tsuno K, Dasgupta R. Melting phase relation of nominally anhydrous, carbonated pelitic-eclogite at 2.5–3.0 GPa and deep cycling of sedimentary carbon. Contrib Mineral Petrol, 2011, 161: 743–763
34 Woodland A B, Koch M. Variation in oxygen fugacity with depth in the upper mantle beneath the Kaapvaal craton, South Africa. Earth Planet Sci Lett, 2003, 214: 295–310
35 Frost D J, McCammon C A. The redox state of the Earth's mantle. Annu Rev Earth Planet Sci, 2008, 36: 389–420
36 Stagno V, Frost D J. Carbon speciation in the asthenosphere: Experimental measurements of the redox conditions at which carbonate-bearing melts coexist with graphite or diamond in peridotite assemblages. Earth Planet Sci Lett, 2010, 300: 72–84
37 Rohrbach A, Schmidt M W. Redox freezing and melting in the Earth's deep mantle resulting from carbon-iron redox coupling. Nature, 2011, 472: 209–212
38 Yin Q P. How is the diamand created (in Chinese). Jewel Sci Technol, 2004, 16: 44–50
39 Lowenstern J B. Carbon dioxide in magmas and implications for hydrothermal systems. Miner Depos, 2001, 36: 490–502
40 Dixon J E. Degassing of alkalic basalts. Am Mineral, 1997, 82: 368–378
41 Lesne P, Scaillet B, Pichavant M, et al. The carbon dioxide solubility in alkali basalts: An experimental study. Contrib Mineral Petrol, 2011, 162: 153–168
42 Rea D K, Ruff L J. Composition and mass flux of sediment entering the world's subduction zones: Implications for global sediment budgets, great earthquakes, and volcanism. Earth Planet Sci Lett, 1996, 140: 1–12
43 Shen X J, Zhang L F. Current research progress in petrology of carbonated eclogites (in Chinese). Earth Sci Front, 2009, 16: 374–384
44 Johnston F K B, Turchyn A V, Edmonds M. Decarbonation efficiency in subduction zones: Implications for warm Cretaceous climates. Earth Planet Sci Lett, 2011, 303: 143–152
45 Plank T, Langmuir C H. The chemical composition of subducting sediment and its consequences for the crust and mantle. Chem Geol, 1998, 145: 325–394
46 Carlson R L, Herrick C N. Densities and porosities in the oceanic crust and their variations with depth and age. J Geophys Res, 1990, 95: 9153–9170
47 Reymer A, Schubert G. Phanerozoic addition rates to the continental crust and crustal growth. Tectonics, 1984, 3: 63–77
48 Marty B, Tolstikhin I N. CO_2 fluxes from mid-ocean ridges, arcs and plumes. Chem Geol, 1998, 145: 233–248
49 Wang C Y. Density and constitution of the mantle. J Geophys Res, 1970, 75: 3264–3284
50 Hayes J M, Waldbauer J R. The carbon cycle and associated redox processes through time. Phil Trans R Soc B, 2006, 361: 931–950
51 Hilton D R, Fischer T P, Marty B. Noble gases and volatile recycling at subduction zones. Rev Mineral Geochem, 2002, 47: 319–370
52 Sano Y, Williams S N. Fluxes of mantle and subducted carbon along convergent plate boundaries. Geophys Res Lett, 1996, 23: 2749–2752
53 Ingebritsen S E, Manning C E. Diffuse fluid flux through orogenic belts: Implications for the world ocean. Proc Nat Acad Sci USA, 2002, 99: 9113–9116
54 Blundy J, Cashman K V, Rust A, et al. A case for CO_2-rich arc magmas. Earth Planet Sci Lett, 2010, 290: 289–301
55 Bulanova G P, Walter M J, Smith C B, et al. Mineral inclusions in sublithospheric diamonds from Collier 4 kimberlite pipe, Juina, Brazil: subducted protoliths, carbonated melts and primary kimberlite magmatism. Contrib Mineral Petrol, 2010, 160: 489–510
56 Muehlenbachs K, Byerly G. ^{18}O-Enrichment of silicic magmas caused by crystal fractionation at the Galapagos Spreading Center. Contrib Mineral Petrol, 1982, 79: 76–79
57 Teng F Z, Dauphas N, Helz R T. Iron isotope fractionation during magmatic differentiation in Kilauea Iki lava lake. Science, 2008, 320: 1620–1622
58 Schuessler J A, Schoenberg R, Sigmarsson O. Iron and lithium isotope systematics of the Hekla volcano, Iceland—Evidence for Fe isotope fractionation during magma differentiation. Chem Geol, 2009, 258: 78–91
59 Teng F Z, Wadhwa M, Helz R T. Investigation of magnesium isotope fractionation during basalt differentiation: Implications for a chondritic composition of the terrestrial mantle. Earth Planet Sci Lett, 2007, 261: 84–92
60 Liu S A, Teng F Z, He Y S, et al. Investigation of magnesium isotope fractionation during granite differentiation: Implication for Mg isotopic composition of the continental crust. Earth Planet Sci Lett, 2010, 297: 646–654
61 Amini M, Eisenhauer A, Böhm F, et al. Calcium isotopes ($\delta^{44/40}Ca$) in MPI-DING reference glasses, USGS rock powders and various rocks: Evidence for Ca isotope fractionation in terrestrial silicates. Geostand Geoanal Res, 2009, 33: 231–247
62 Schidlowski M. A 3800-million-year isotopic record of life from carbon in sedimentary rocks. Nature, 1988, 333: 313–318
63 Cartigny P. Stable isotopes and the origin of diamond. Elements, 2005, 1: 79–84
64 Walter M J, Kohn S C, Araujo D, et al. Deep mantle cycling of oceanic crust: Evidence from diamonds and their mineral inclusions. Science, 2011, 334: 54–57
65 Lupton J E. Terrestrial inert gases-Isotope tracer studies and clues to primordial components in the mantle. Ann Rev Earth Planet Sci, 1983, 11: 371–414
66 Sano Y, Marty B. Origin of carbon in fumarolic gas from island arcs. Chem Geol, 1995, 119: 265–274
67 Sano Y, Gamo T, Williams S N. Secular variations of helium and carbon isotopes at Galeras volcano, Colombia. J Volcanol Geotherm Res, 1997, 77: 255–265
68 Hilton D R, Craig H. A helium isotope transect along the Indonesian archipelago. Nature, 1989, 342: 906–908
69 Milliman J D. Production and accumulation of calcium carbonate in the ocean: Budget of a nonsteady state. Global Biogeochem Cycles, 1993, 7: 927–957
70 Chang V T C, Williams R J P, Makishima A, et al. Mg and Ca isotope fractionation during $CaCO_3$ biomineralisation. Biochem Biophys Res Commun, 2004, 323: 79–85
71 Galy A, Yoffe O, Janney P E, et al. Magnesium isotope heterogeneity of the isotopic standard SRM980 and new reference materials for magnesium-isotope-ratio measurements. J Anal At Spectrom, 2003, 18: 1352–1356
72 Wombacher F, Eisenhauer A, Böhm F, et al. Magnesium stable isotope fractionation in marine biogenic calcite and aragonite. Geochim Cosmochim Acta, 2011, 75: 5797–5818

73 Li W Y, Teng F Z, Xiao Y L, et al. High-temperature inter-mineral magnesium isotope fractionation in eclogite from the Dabie orogen, China. Earth Planet Sci Lett, 2011, 304: 224–230
74 Chavagnac V, Jahn B M. Coesite-bearing eclogites from the Bixiling complex, Dabie Mountains, China: Sm-Nd ages, geochemical characteristics and tectonic implications. Chem Geol, 1996, 133: 29–51
75 Zhang R Y, Liou J G, Cong B L. Talc-, magnesite- and Ti-clinohumite-bearing ultrahigh-pressure meta-mafic and ultramafic complex in the Dabie Mountains, China. J Petrol, 1995, 36: 1011–1037
76 Yang W, Teng F Z, Zhang H F, et al. Magnesium isotopic systematics of continental basalts from the North China craton: Implications for tracing subducted carbonate in the mantle. Chem Geol, 2012, doi: 10.1016/j.chemgeo.2012.05.018
77 Anderson D L. Chemical composition of the mantle. J Geophys Res, 1983, 88(Suppl): B41–B52
78 Eisenhauer A, Nägler T F, Stille P, et al. Proposal for an international agreement on Ca notation as a result of the discussion from the workshop on stable isotope measurements in Davos (Goldschmidt 2002) and Nice (EGS-AGU-EUG 2003). Geostand Geoanal Res, 2004, 28: 149–151
79 Farkaš J, Buhl D, Blenkinsop J, et al. Evolution of the oceanic calcium cycle during the late Mesozoic: Evidence from $\delta^{44/40}$Ca of marine skeletal carbonates. Earth Planet Sci Lett, 2007, 253: 96–111
80 Holmden C. Ca isotope study of Ordovician dolomite, limestone, and anhydrite in the Williston Basin: Implications for subsurface dolomitisation and local Ca cycling. Chem Geol, 2009, 268: 180–188
81 DePaolo D J. Calcium isotopic variations produced by biological, kinetic, radiogenic and nucleosynthetic processes. Rev Mineral Geochem, 2004, 55: 255–288
82 Huang S C, Farkaš J, Jacobsen S B. Calcium isotopic fractionation between clinopyroxene and orthopyroxene from mantle peridotites. Earth Planet Sci Lett, 2010, 292: 337–344
83 Simon J I, DePaolo D J. Stable calcium isotopic composition of meteorites and rocky planets. Earth Planet Sci Lett, 2010, 289: 457–466
84 De La Rocha C L, DePaolo D J. Isotopic evidence for variations in the marine calcium cycle over the Cenozoic. Science, 2000, 289: 1176–1178
85 Fantle M S, DePaolo D J. Variations in the marine Ca cycle over the past 20 million years. Earth Planet Sci Lett, 2005, 237: 102–117
86 Gussone N, Böhm F, Eisenhauer A, et al. Calcium isotope fractionation in calcite and aragonite. Geochim Cosmochim Acta, 2005, 69: 4485–4494